

Measurements of acoustic streaming in a looped-tube thermoacoustic engine with a jet pump

著者	琵琶 哲志
journal or publication title	Journal of Applied Physics
volume	101
number	6
page range	064914
year	2007
URL	http://hdl.handle.net/10097/46580

doi: 10.1063/1.2713360

Measurements of acoustic streaming in a looped-tube thermoacoustic engine with a jet pump

Tetsushi Biwa

Department of Mechanical Systems and Design, Tohoku University, Aoba-ku, Sendai 980-0013, Japan

Yusuke Tashiro

Department of Crystalline Materials Science, Nagoya University, Chikusa-ku, Nagoya 464-8603, Japan

Masahiro Ishigaki

Department of Computational Science and Engineering, Nagoya University, Chikusa-ku, Nagoya 464-8603, Japan

Yuki Ueda

Graduate School of Bio-applications and Systems Engineering, Tokyo University of Agriculture and Technology, Naka-cho, Koganei, Tokyo 184-8588, Japan

Taichi Yazaki

School of Physics, Aichi University of Education, Igaya-cho, Kariya-City 448-8542, Japan

(Received 9 July 2006; accepted 21 January 2007; published online 30 March 2007)

This paper reports on the acoustic streaming in a looped-tube thermoacoustic prime mover equipped with an asymmetric constriction called a jet pump. The time-averaged mass flow velocity was determined using visualization methods and using acoustic field measurements. It was demonstrated that the magnitude and the direction of the velocity were dependent on the orientation of the jet pump. From the observed velocities, we estimated the heat carried away from the hot heat exchanger by the mass flow. It was shown that the heat loss was decreased from 30 W to 6.5 W by reversing the orientation of the jet pump, when the input heat power supplied to the prime mover was 100 W. The influence of the acoustic streaming was also studied from the cooling temperature of the looped-tube cooler. © 2007 American Institute of Physics. [DOI: 10.1063/1.2713360]

I. INTRODUCTION

Many thermoacoustic heat engines are being developed using a looped tube with a regenerator,¹⁻⁴ instead of a resonator with a stack. This is because the acoustic wave running around the loop executes a thermodynamic cycle that is similar to the Stirling cycle in the regenerator. The Stirling cycle can ideally achieve the efficiency of Carnot's cycle. Therefore, thermoacoustic Stirling heat engines can offer efficiency that is comparable to that of conventional heat engines.⁴ On the other hand, it has been pointed out that the looped tube allows a nonzero mass flow to circulate through the loop.⁵

The time-averaged mass flow velocity caused by the acoustic streaming is expressed as

$$V_m = U_m + v, \quad (1)$$

where U_m is the Eulerian average of the velocity. This term is zero when the acoustic wave is absent.⁶⁻⁹ The velocity v is given as $v = \langle \rho U \rangle / \rho_m$; ρ and U , respectively, represent the oscillating density and velocity; angular brackets represent the time average; and ρ_m is mean density. The mass flow circulating through the loop carries heat away from the hot heat exchangers in the prime mover, and adds an additional heat load to the cold heat exchanger in the cooler, both of which result in unwanted heat losses.

To control the mass flow velocity V_m in the loop, Backhaus and Swift proposed the use of a geometrically asymmetric constriction called a "jet pump."^{3,4} Hydrody-

namic end effects generate different mean pressures at the two ends of the jet pump. This pressure drop creates a steady counter-flow which can suppress the total mass flow, but the energy loss, called a "minor loss," is unavoidable in the jet pump.^{10,11} In addition to the measurements of the acoustic output power,^{1,2,12,13} it becomes important to address both the mass flow velocity and the energy loss in the jet pump simultaneously in the study of thermoacoustic Stirling prime movers.

In this work, we built a looped-tube thermoacoustic Stirling prime mover with a jet pump. Using visualization methods and using acoustic field measurements,¹⁴ we show how the velocities V_m , U_m , and v change when the orientation of the jet pump is reversed. The energy loss associated with the jet pump is shown by the axial distribution of the acoustic power flow. To demonstrate the influence of the mass flow on the cooler, the cooling power is shown in a looped-tube thermoacoustic Stirling cooler constructed from the present prime mover.

II. EXPERIMENTS

A. Experimental setup

A schematic illustration of the present thermoacoustic prime mover is shown in Fig. 1(a). The direction of the gravitational acceleration g is shown as a thick arrow. The loop had an average length of 2.1 m and was made of glass and stainless steel tubes having an inner diameter of 40 mm. These tubes were joined by three elbows and a tee at one

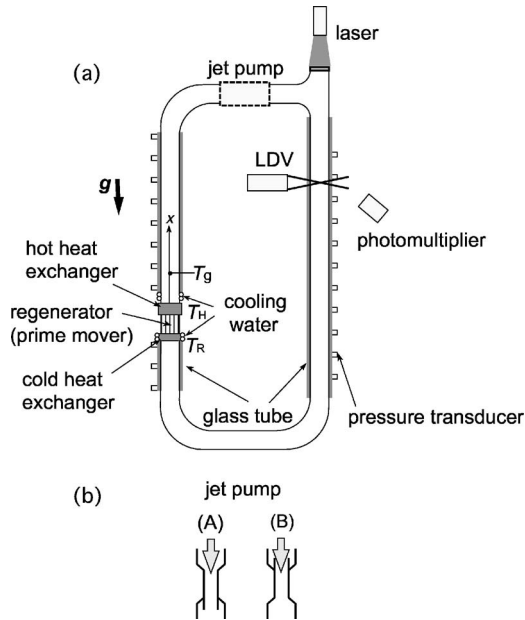


FIG. 1. Schematic illustration of the looped-tube thermoacoustic engine (a) with jet pump (b) installed. The position at which gas temperature T_g is measured is shown as a dot.

corner. One end of the tee was closed with a glass plate, through which a sheetlike plane of light from an Ar-ion laser (500 mW) was introduced into the glass tube.

The jet pump was made out of a narrow tube with 24 mm inner diameter and 65 mm length. The ends of the tube were tapered with conical waveguides, giving the jet pump a total length of 75 mm. Figure 1(b) shows that one end of the narrow tube was extended into the inside of the cone, but the other end was connected to the cone smoothly without an abrupt change in the cross section. The largest inner diameter of the cone is 40 mm, which is equal to that of the straight tubes. The jet pump was installed in the velocity maximum, (shown as a dashed region in the loop) because the critical heat power, above which the spontaneous gas oscillation was excited, was minimized. The jet pump was installed in two orientations: in the first orientation, (A), the acoustic power flows into the jet pump from the “smooth” end. In the second orientation, (B), the acoustic power flows out of the smooth end.

A prime-mover regenerator consisting of a ceramic honeycomb with many square channels of cross section $0.9 \times 0.9 \text{ mm}^2$ was sandwiched by two heat exchangers consisting of strips aligned in parallel to the oscillating flow. An electrical heater heated one heat exchanger and a thermocouple monitored its temperature T_H . In addition, the temporal mean temperature T_g of the gas, on the central axis of the tube and 9 cm above the hot heat exchanger, was monitored to elucidate the mass flow qualitatively.⁹ The second heat exchanger was kept at room temperature $T_R (=15 \text{ }^\circ\text{C})$ using cooling water. The cooling water was also used to maintain the temperature of the stainless steel tube near the hot heat exchanger at T_R .

B. Preliminary measurements of streaming

The present experimental setup was filled with air at atmospheric pressure. When the heat power Q_H generated by

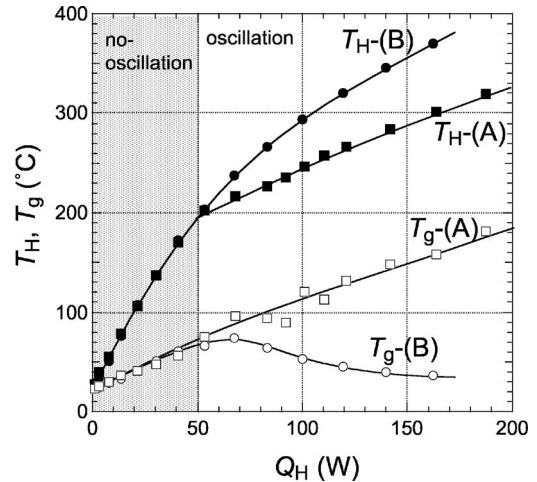


FIG. 2. Q_H -dependence of the hot heat exchanger temperature T_H and the gas temperature T_g . Also, T_H and T_g are shown as solid and open squares when jet pump (a) is used, and by circles when jet pump (b) is used.

the electrical heater was greater than 50 W, the gas column in the loop began to oscillate at the fundamental mode with the frequency f of 146 Hz, independently of the orientations (A) and (B) of the jet pump. The mass flow was studied preliminarily using temperature measurements.

Figure 2 shows the hot heat exchanger temperature T_H and the gas temperature T_g as a function of Q_H . Initially, the temperatures T_g and T_H , both start to increase with increasing Q_H . The increase of T_g is attributed mainly to thermal convection, because the loop stands vertically, parallel to the direction of g . However, in the region above $Q_H=50 \text{ W}$, T_g with jet pump (B) starts to decrease in response to excitation of the spontaneous gas oscillation, whereas T_g with jet pump (A) continues to increase. On the other hand, the hot heat exchanger temperature T_H with jet pump (B) becomes higher than T_H with (A) when the oscillation is present with $Q_H > 50 \text{ W}$.

The lower T_H and the higher T_g observed with (A) imply that the mass flow rises from the hot heat exchanger; the mass flow heated by the hot heat exchanger passes through the position where T_g is monitored. It is also suggested that when jet pump (B) is used, the clockwise mass flow is suppressed and its direction is reversed because the gas temperature T_g starts to decrease to the room temperature T_R . To verify these inferences obtained from temperature measurements, we directly measured acoustic streaming through visualization and acoustic field measurements. Differences in T_H and T_g caused by the orientation of the jet pump are readily apparent with any Q_H beyond 50 W. Therefore, Q_H was set to 100 W as the heating condition in the following measurements.

C. Experimental procedure

1. Visualization

Tracer particles of 8 μm in typical diameter were introduced into the glass tube, and visualized using a sheetlike Ar-ion laser light. Motion of the tracer particles on the plane sliced by the sheet of light was recorded with a digital video

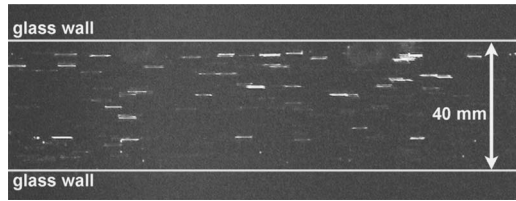


FIG. 3. Visualization of the mass flow near $x=1.36$ m. Bright lines represent traces of the oscillating tracer particles. Thick horizontal lines represent the tube wall.

camera.¹² By tracking a specific tracer particle, the Lagrangian velocities are visible in this experimental method.

The loop was laid horizontally on the desk in the visualization, to observe the axial velocity separately from the particle fall velocity. Instead, the loop stood vertically during temperature measurements described in the preceding section and the pressure and velocity measurements shown below. Consequently, the contribution of the thermal convection to the mass flow was suppressed in this measurement, more so than in the case when the loop stood vertically.

2. Acoustic field measurement

Acoustic pressure $P=p \exp(i\omega t)$ ($\omega=2\pi f$) was measured using a series of small pressure transducers mounted on the glass tube walls. The axial velocity was measured on the central axis of the tube using a laser Doppler velocimeter (LDV).¹⁵ The LDV monitors the velocity U_m+U of the gas passing through a fixed position where two laser beams form an interference fringe. Hence, the time average of the measured velocity gives the Eulerian average of the velocity U_m .¹⁶

We also obtained the oscillating velocity U by the LDV measurements, and converted it into the cross-sectional average \bar{U} using the theoretical solution for a laminar oscillating flow.¹⁷ The acoustic power is given as

$$I = A \langle P\bar{U} \rangle = \frac{1}{2} A p u \cos \varphi, \quad (2)$$

where A is the cross-sectional area of the tube, and $\bar{U} = u \exp i(\omega t + \varphi)$ represents the oscillating part of the cross-sectional mean velocity.

III. EXPERIMENTAL RESULTS

A. Visualization of streaming

Figure 3 depicts one image taken from the video. The traces of the individual particles are seen as horizontal straight lines because of the slower shutter speed than the acoustic period ($=1/146$ s). The lines moved along the tube axis with a steady velocity. This is the time-averaged mass flow velocity V_m , called the Lagrangian average of the velocity.¹⁶

The mass flow velocity V_m was determined from the videos recorded when jet pumps (A) and (B) were used. Measurements indicated that V_m near the centerline of the tube was 44 mm/s in the *clockwise* direction when jet pump (A) was used. On the other hand, V_m was 32 mm/s in the *counter-clockwise* direction with jet pump (B) installed. This

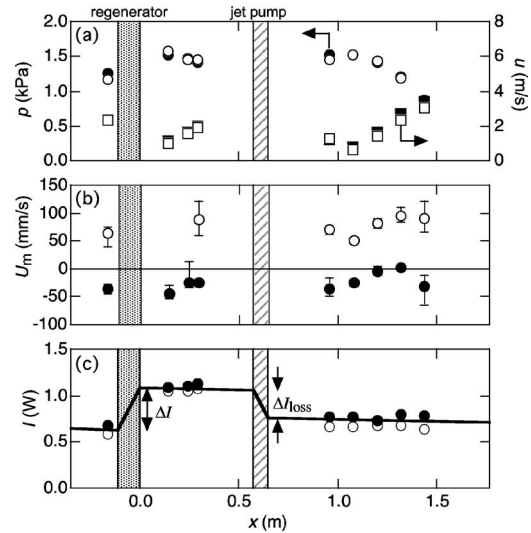


FIG. 4. Acoustic fields in the present looped-tube engine: (a) pressure amplitude p (open circle and filled circle) and the cross-sectional average velocity amplitude u (open square and filled square); (b) Eulerian average U_m of the velocity; and (c) acoustic power I . Open and solid symbols, respectively, represent data with jet pumps (a) and (b). The regenerator and the jet pump are shown, respectively, as dotted and shaded regions.

is a direct demonstration that the jet pump can control the velocity and the direction of the mass flow as a result of its asymmetric constriction.

For a rough estimation of the heat leak, Q_{leak} , caused by the mass flow we express the total mass flow over the cross section of the tube as $A\rho_m V_m$, and obtain the heat leak in the following form:³

$$Q_{\text{leak}} = A\rho_m |V_m| C_p \Delta T, \quad (3)$$

where C_p is the isobaric specific heat of the gas per unit mass, and $\Delta T = T_H - T_R$. Results demonstrate that $Q_{\text{leak}} = 18$ W with jet pump (A), and $Q_{\text{leak}} = 13$ W with jet pump (B). These heat leaks are 18% and 13% of the input heat power $Q_H = 100$ W, and therefore, markedly impair the performance of the looped-tube engine.

B. Pressure and velocity fields

The pressure p and velocity u amplitudes obtained when $Q_H = 100$ W are shown as a function of the axial coordinate x in Fig. 4(a), where the regenerator is shown as a dotted region and the jet pump by a hatched one. The coordinate x is directed clockwise in the loop from the hot heat exchanger ($x=0$). The regenerator is positioned near the pressure maximum¹⁸ and the jet pump is positioned at the velocity maximum, independently of the jet pump orientation.

A clear difference was observed in the Eulerian average U_m of the velocity on the central axis of the tube. Figure 4(b) shows that U_m with jet pump (A) installed is 50–100 mm/s, meaning that U_m is always directed in a clockwise direction. On the other hand, U_m with jet pump (B) installed ranges from -50 to 0 mm/s, indicating a velocity in the counter-clockwise direction. Their simple averages in the range $0.96 \text{ m} < x < 1.44 \text{ m}$ were $U_m = 77$ mm/s with jet pump (A), and $U_m = -19$ mm/s with jet pump (B). Therefore,

the orientation of the jet pump strongly affects the Eulerian average U_m of the velocity without changing the axial distribution of p and u .

C. Acoustic power

The acoustic power I is shown in Fig. 4(c). The obtained I is always positive, showing that I flows in the clockwise direction in the loop. The increase, ΔI , in the regenerator is 0.5 W, which represents the output power resulting from the thermoacoustic energy conversion. Because the phase lead ϕ of the velocity to the pressure was 25° , close to a traveling wave phase, the present looped-tube engine acts as a thermoacoustic Stirling prime mover.¹⁸ The hot heat exchanger temperature T_H equals 251°C when jet pump (A) is installed. With jet pump (B) installed T_H is 289°C , which is higher than that of jet pump (A). However, the magnitude of ΔI is independent of the jet pump orientation. This fact indicates that the output power ΔI of the prime mover is not given merely by the temperatures at the both ends; it is also affected by the mass flow velocity in the loop.¹⁹

The acoustic power emitted from the hot heat exchanger decreases in the jet pump. This drop of I shows the acoustic power dissipation in the jet pump called “minor loss.” The magnitude of the minor loss is so great that more than 60% of the output power ΔI is consumed in the jet pump regardless of its orientation. The remaining part of the output power compensates for the surface attenuation resulting from the viscosity and thermal conduction of the gas in the glass tube with a constant cross-sectional area. The dissipative energy per unit length in the jet pump is 4.1 W/m, but it is below 0.1 W/m in the glass tube, meaning that the minor loss induced by the abrupt change in the cross-section can become much greater than the surface attenuation.

D. Mass flow velocity

In this section, we estimate the mass flow velocities $v = \langle \rho U \rangle / \rho_m$ and V_m from the acoustic field measurements. The thermal penetration depth δ_α is 0.30 mm in the present setup at room temperature²⁰ and the glass tube radius is 20 mm. Therefore, we can safely assume the wave is adiabatic, and the relation $\rho = P/c^2$ holds for the oscillating density ρ and pressure P , where c is the adiabatic sound speed. In addition, the viscous penetration depth δ_ν is 0.18 mm,²⁰ which is much smaller than the tube radius. Hence, the oscillating velocity can be regarded as uniform in the cross section of the glass tube.¹⁷ From these simplifications, the mass flow velocity v is expressed using the acoustic power I as

$$v = I / (A \rho_m c^2). \quad (4)$$

We obtained $v = 4$ mm/s in the clockwise direction by inserting $I = 0.7$ W as a typical value, which is much smaller than U_m observed with the LDV.

Now we are ready to determine the mass flow velocity V_m . Inserting into Eq. (1) the values $v = 4$ mm/s and $U_m = 77$ mm/s for jet pump (A) and -19 mm/s for jet pump (B), we obtain $V_m = 81$ mm/s for jet pump A and $V_m = -15$ mm/s for jet pump B. These mass flow velocities V_m are quantitatively different from the values obtained using the

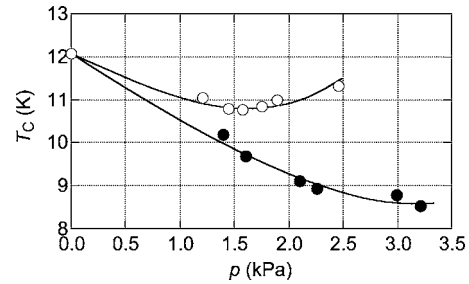


FIG. 5. Cooling temperature T_c vs pressure amplitude p . Open and solid symbols respectively represent data with jet pumps (a) and (b). Solid lines are guides for the eye.

visualization method, which were $V_m = 44$ mm/s for jet pump (A) and -32 mm/s for jet pump (B). We attribute the differences in V_m values to the degree of the contribution of the thermal convection to the mass flow, because the orientation of the loop with regard to g is different in these measurements.

We inserted the mass flow velocity $V_m = U_m + v$ into Eq. (3), and estimated the heat leaks. Results showed that $Q_{\text{leak}} = 30$ W with jet pump (A), and $Q_{\text{leak}} = 6.5$ W with (B). The jet pump appears to affectively control mass flow velocity V_m and the associated heat leak Q_{leak} . On the other hand, more than 60% of the acoustic output power ΔI is consumed in the jet pump as the minor loss. Therefore, careful control of both the acoustic streaming and the minor loss is important for upgrading the performance of thermoacoustic Stirling engines.

E. Looped-tube cooler equipped with a jet pump

To investigate the influence of the mass flow on cooling performance, we built a looped-tube cooler by modifying the experimental setup shown in Fig. 1. A ceramic honeycomb sandwiched by two heat exchangers was installed in the loop as a cooler regenerator in such a way that the traveling wave phase and the highest acoustic impedance were achieved in it.^{2,12} The traveling wave gives rise to an acoustic heat flow opposite to the direction of I in the cooler regenerator. For that reason, the heat exchanger temperature at the downstream side of I was monitored as the cooling temperature T_c of this cooler. The heat exchanger temperature at the upstream side was maintained at the temperature T_R using running water. In this measurement, the tee used for visualization was replaced with a 90° elbow.

Figure 5 shows the cooling temperature T_c as a function of the maximum pressure amplitude p in the loop. The cooling temperature obtained using jet pump (A) shows a minimum and starts to increase at pressures greater than $p = 1.6$ kPa. A similar upturn of T_c was reported for the looped-tube cooler without the jet pump.² On the other hand, when jet pump (B) was used, the cooling temperature decreased monotonically with increasing p . Consequently, the temperature T_c with jet pump (B) was consistently lower than that with (A). This demonstrates the importance of the control of the mass flow in the thermoacoustic Stirling cooler because the mass flow velocity V_m is higher with jet pump (A) than with (B).

IV. SUMMARY

We built a looped-tube thermoacoustic prime mover that has a jet pump, and observed the Lagrangian average V_m of the velocity using visualization methods and using acoustic field measurements. It was shown that both the direction and the magnitude of V_m were changed with the orientation of the jet pump. The heat leak Q_{leak} due to the steady mass flow was estimated using the observed velocity. It was found that Q_{leak} was 30 W in the first orientation and was 6.5 W in the second orientation, when the heat power Q_H of 100 W was supplied to the prime mover. On the basis of this observation, we constructed a looped-tube thermoacoustic cooler having a jet pump. The cooling temperature is lowered when the mass flow velocity is reduced by the jet pump. Mass flow control is important for upgrading the performance of thermoacoustic Stirling heat engines.

ACKNOWLEDGMENT

This work was supported by Grand-in-Aid for Scientific Research from Japan Society for Promotion of Science.

¹T. Yazaki, A. Iwata, T. Maekawa, and A. Tominaga, *Phys. Rev. Lett.* **81**, 3128 (1998).

²T. Yazaki, T. Biwa, and A. Tominaga, *Appl. Phys. Lett.* **80**, 157 (2002).

³G. W. Swift, D. L. Gardner, and S. Backhaus, *J. Acoust. Soc. Am.* **105**, 711 (1999).

⁴S. Backhaus and G. W. Swift, *Nature* **399**, 335 (1999); *J. Acoust. Soc. Am.*

107, 3148 (2000).

⁵D. Gedeon, *Cryocoolers 9*, edited by R. G. Ross (Plenum Press, New York, 1997), p. 385.

⁶G. W. Swift, *Thermoacoustics: A Unifying Perspective for Some Engines and Refrigerators* (Acoustical Society of America Publications, Sewickley, PA, 2002).

⁷V. Gusev, S. Job, H. Bailliet, P. Lotton, and M. Bruneau, *J. Acoust. Soc. Am.* **108**, 934 (2000).

⁸H. Bailliet, V. Gusev, R. Raspet, and R. A. Hiller, *J. Acoust. Soc. Am.* **110**, 1808 (2001).

⁹S. Job, V. Gusev, P. Lotton, and M. Bruneau, *J. Acoust. Soc. Am.* **113**, 1892 (2003).

¹⁰A. Petculescu and L. A. Wilen, *J. Acoust. Soc. Am.* **113**, 1282 (2003).

¹¹B. L. Smith and G. W. Swift, *J. Acoust. Soc. Am.* **113**, 2455 (2003).

¹²Y. Ueda, T. Biwa, U. Mizutani, and T. Yazaki, *Appl. Phys. Lett.* **81**, 5252 (2002); *J. Acoust. Soc. Am.* **115**, 1134 (2004).

¹³T. Biwa, Y. Tashiro, U. Mizutani, M. Kozuka, and T. Yazaki, *Phys. Rev. E* **69**, 066304 (2004).

¹⁴T. Biwa, M. Ishigaki, Y. Tashiro, Y. Ueda, and T. Yazaki, in *Innov. Nonlin. Acoust.*, ISNA 17, AIP Conf. Proc. **838**, State College, PA, 2006, pp. 395–398.

¹⁵Cigarette smoke was used as seeding particles in LDV.

¹⁶W. L. Nyborg, in *Nonlinear Acoustics*, edited by M. F. Hamilton and D. T. Blackstock (Academic Press Inc., San Diego, 1998), Chap. 7.

¹⁷T. Biwa, Y. Ueda, H. Nomura, U. Mizutani, and T. Yazaki, *Phys. Rev. E* **72**, 026601 (2005).

¹⁸Y. Ueda, T. Biwa, U. Mizutani, and T. Yazaki, *J. Acoust. Soc. Am.* **117**, 3369 (2005).

¹⁹G. Penelet, V. Gusev, P. Lotton, and M. Bruneau, *Phys. Lett. A* **351**, 268 (2006).

²⁰The thermal penetration depth δ_α is expressed as $\sqrt{2\alpha/\omega}$, where α denotes thermal diffusivity and $\omega=2\pi f$ is the angular frequency. The viscous penetration depth δ_ν is expressed as $\delta_\alpha\sqrt{\sigma}$, where σ is the Prandtl number.